

Karl-Friedrich Berger,  
Sandra Kiefer (Hrsg.)

# **JAHRBUCH 2024**

Dichten. Kleben. Polymer.

# Estimating the contact temperature and the pumping rate of rotary shaft seals

## New possibilities with an web application

**CROSS-INDUSTRY** – In many applications of rotary shaft seals, engineers want to know about the risk of thermal damaging or leakage due to a low back pumping capability. Both aspects – thermal damaging as well as the back pumping capability – are affected by many influencing factors that also interact with each other. Therefore, precise and robust answers often require time-consuming and expensive test-runs. However, neglecting some influencing factors of minor importance, much faster but still valid answers can be obtained. With this objective, the web application IMA-InsECT has been developed as a free and easy-to-use tool.

### Introduction

Many applications require seals that retain lubricants or other fluids within machines and prevent the entry of dirt into these machines. In applications with rotating shafts, mostly rotary shaft lip-type seals are used [1, 2]. The rotary shaft seal, the surface of the shaft and the fluid, which has to be sealed (often oil), form a dynamic sealing system representing a tribological system [3] that is significantly affected by its periphery and the operating conditions. Elastomeric rotary shaft lip-type seals are standardised in national and international standards, [4, 5, 6]. They consist of a metal insert to which a sealing lip is attached (**Fig. 1**). During assembly, the sealing lip and a garter spring are widened by the shaft. The garter spring provides the



Von Simon Feldmeth,  
Team Manager Simulation,  
Sumbat Bekgulyan,  
Research Assistant at IMA until June 2022

University of Stuttgart, Institute of Machine  
Components (IMA)  
<http://www.ima.uni-stuttgart.de>



Professor Dr.-Ing. habil. Frank Bauer,  
Head of Sealing Technology



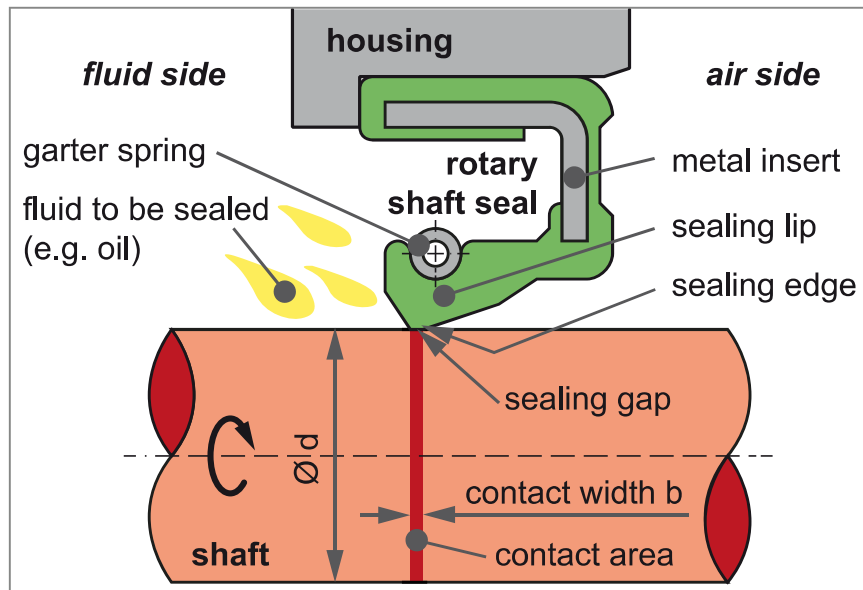


**Fig. 1: Sealing system consisting of rotary shaft seal, shaft and fluid [7]**

(Fig.: University of Stuttgart)

necessary contact pressure under all operating conditions. The sealing lip is pressed against the shaft surface, forming a slim contact area between its sealing edge and the shaft. The width of the contact area is approximately  $b = 0.1$  to  $0.2$  mm. The average contact pressure in the contact area is about 1 MPa.

### Operating principle

During the dynamic operation, the fluid enters the contact area between the sealing edge and the rotating shaft. Thereby, a sealing gap, which is filled with fluid, is formed between the sealing edge and the shaft surface (**Fig. 2**). Due to the different lip face angles  $\alpha$  and  $\beta$  an asymmetric pressure distribution results in the contact area. Additionally, the rough elastomer surface of the sealing edge deforms elastically in circumferential direction while sliding on the shaft surface. Mainly the combination of these processes in the contact area results in an active back pumping capability, which prevents the fluid from leaking out of the sealing gap. Furthermore, there are other operating principles explaining the active back pumping capability of rotary shaft seals in more detail [8].

### Pumping rate

The active back pumping capability can be observed by offering fluid to the rotary shaft seal on the air side. The offered fluid is pumped from the air side to the fluid side. The quotient of the pumped fluid quantity and the elapsed time equals the pumping rate, which describes the back pumping capability quantitatively. Pumping rate measurements can show the influence of individual system parameters on the leak-tightness of rotary shaft seals, [9, 10, 11, 12, 13, 14, 15].

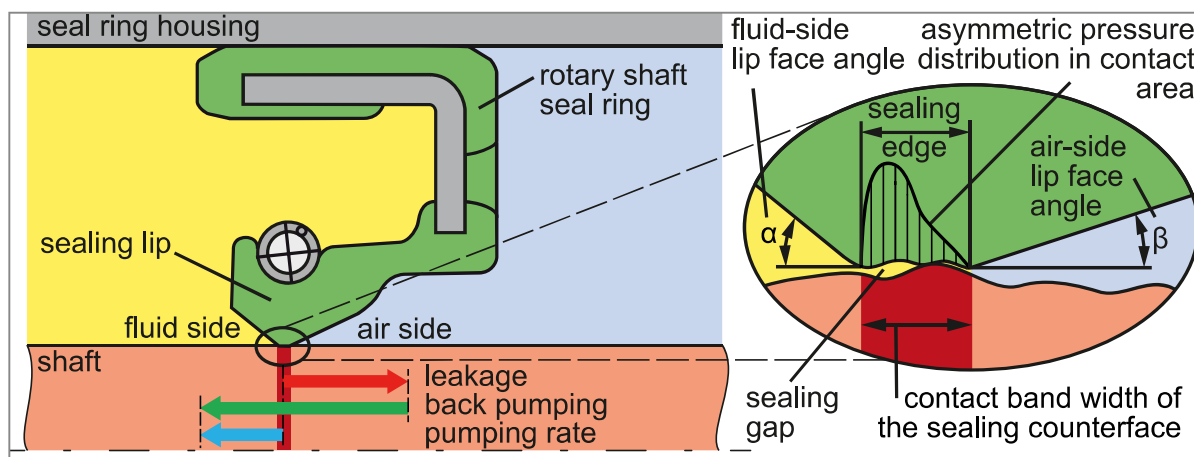


**Fig. 2: Sealing mechanism of rotary shaft seals according to [8]** (Fig.: University of Stuttgart)

There are several test methods to measure the pumping rate of a sealing system, e.g. [8, 9, 10, 11, 12, 13, 14, 15]. All these methods are based on two measuring principles. Either the amount of pumped fluid (mass or volume) for a certain period of time (principle 1) or the time required to pump a certain amount of fluid (principle 2) is measured. The pumping rate can be normalised for the comparison of sealing systems with different shaft speeds or with different shaft diameters.

Often, the pumping rate is given in  $\mu\text{l}/\text{m}$  as the pumped fluid volume per sliding distance on the shaft surface according to **Eq. 1**, where  $\Delta m$  represents the mass of the pumped fluid,  $d$  the diameter of the shaft,  $\Delta t$  the pumping time,  $\rho$  the density of the fluid and  $n$  the shaft speed in rpm,

$$\text{pumping rate} = \Delta m / (\pi \cdot d \cdot \Delta t \cdot \rho \cdot n) \quad \text{Eq. 1}$$

In several research projects, analyses for the assessment of the leak-tightness by means of the pumping rate were performed for mineral and synthetic oils [9, 10, 11, 12, 13, 14, 15]. An empirical model for calculating the pumping rate was developed and published as a spreadsheet file [10, 12].

### Frictional heat and contact temperature

Energy is dissipated in the contact area during operation due to friction. This means, kinetic energy is converted to frictional heat. The temperature in the contact area is higher, the more frictional heat is generated and the poorer this heat is transferred away from the contact area. A high contact temperature is very harmful to the sealing system since it accelerates the aging of the elastomer as well as the deposition of oil carbon (**Fig. 3**). Both mechanisms reduce the lifetime of the sealing system since





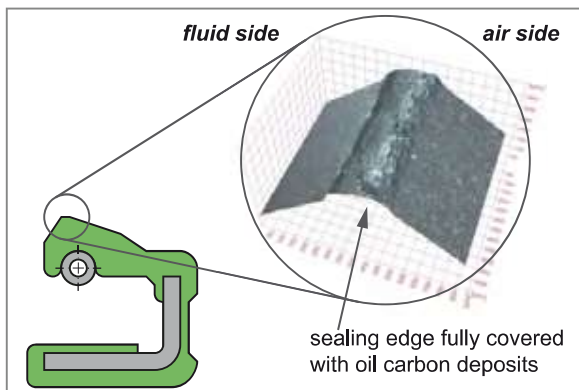


**Fig. 3: Oil carbon deposit on the sealing edge of a rotary shaft seal**

(Fig.: University of Stuttgart)

they deteriorate the deformability and surface of the sealing edge and thus the back-pumping capability of the sealing system.

In order to achieve a long lifetime, moderate temperatures in the sealing system, and especially in the contact area, must be ensured during the development of new machines. A reliable and economic design of the sealing system is only possible if the temperature range in the contact area is known.

The contact temperature of a sealing system depends on its thermal behaviour which is affected by many influencing factors. These influencing factors either affect the heat generation (e.g. the surface topography of the shaft) or the heat dissipation (e.g. the thermal conductivity of the shaft material) or even both (e.g. shaft speed). **Fig. 4** shows the most important influencing factors, their interactions and their effects on the contact temperature.

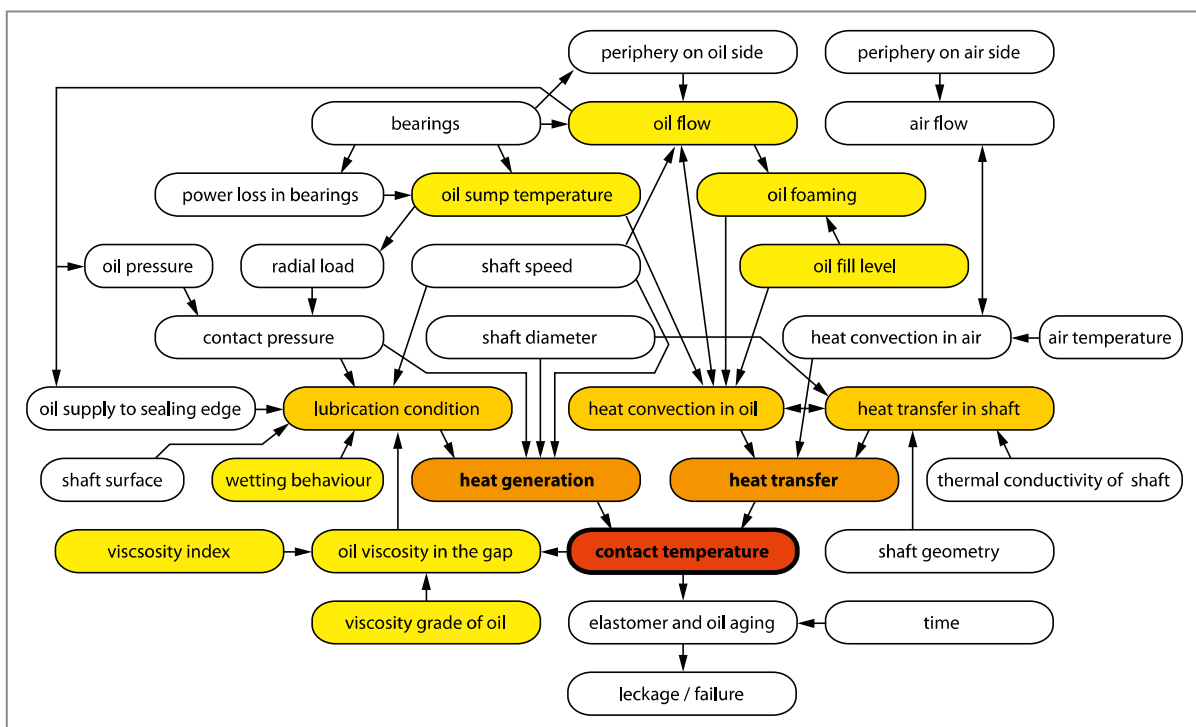


**Fig. 4: Factors influencing the contact temperature [21]** (Fig.: University of Stuttgart)

The contact temperature of a sealing system can be determined either by simulating the fluid flow and heat transfer in the sealing system and its periphery [16, 17, 18] or by measurements during test runs, for example by using pyrometers [19] or thermal imager [20, 21]. These non-contacting measuring methods as well as contacting methods using thermocouples or resistance thermometers are summarised and compared in [7]. In addition to measurements and complex simulations, estimation methods have also been developed. These methods can be quickly used to roughly calculate the contact temperature based on the most relevant operating conditions. The most popular estimation methods are presented and compared in [22].

### The Web application

IMA-InsECT is a tool, that allows to estimate the contact temperature as well as the pumping rate of rotary shaft seals. It is offered free of charge and is accessible online [23]. The calculation is performed on a web server and the user interaction is done via the web page acting as the user interface. The user defines the operating and friction conditions as well as the fluid data via input fields and gets the calculated contact temperature or pumping rate within a fraction of a second as a result in an output field on the IMA-InsECT web page. Additionally, a calculation report containing the results as well as the corresponding input parameters, can be downloaded. The user interface of the web app runs in the browser on any IT devices with internet connection, such as smartphones, tablets, laptops or desktop computers. Thus, the user does not need to install or update any software on his device. The user interface is automatically fitted to the screen size of the device and is available in English and German.

Several toolkits are used for running the IMA-InsECT web server. The most important toolkits are Django [24] providing a high-level Python web framework and Bootstrap [25] offering a powerful, extensible, and feature-packed frontend toolkit. The calculation module is written in Python and is based on the former (offline) desktop version of IMA-InsECT [26] which is no longer supported. **Fig. 5** shows the user-interface of IMA-InsECT for calculating the contact temperature.

### Calculation of the contact temperature with the web application

There are several methods for calculating the temperature rise. In most cases, these methods consist of two steps (**Fig. 6**):

- In the first step, the tool calculates how much frictional heat is generated in the contact area.
- In the second step, the resulting temperature rise is calculated. Since the oil viscosity in the sealing gap and thus the heat generation strongly depends on the contact



The screenshot shows the InsECT web application interface. At the top, a dark navigation bar contains the 'InsECT' logo and menu items: 'Tool', 'Settings', 'Info', 'Manual', 'Imprint', and 'Language'. Below this, the 'Method for temperature rise' is set to 'ExACT equation' and the 'Method for frictional heat' is set to 'Guembel curve friction model'. The 'Operating conditions' section includes input fields for shaft speed (3000,0 rpm), shaft diameter (80,0 mm), relative fluid fill level (50,0 %), fluid sump temperature (80,0 °C), thermal conductivity of shaft (43,0 W/(m·K)), and temperature of the ambient air (20,0 °C). There are also sections for 'Friction conditions' and 'Fluid data'. At the bottom, there are 'Calculate!' and 'Reset input parameters' buttons. A 'Results' section displays: temperature rise ≈ 44,4 K, contact temperature ≈ 124,4 °C, circumferential speed ≈ 12,6 m/s, and thermal resistance ≈ 79,79 m·K/W. A 'Download report' button is located below the results. Red arrows point to the main menu, method selection dropdowns, input fields, the results box, and the download report button.

**main menu**

**method selection for temperature rise and frictional heat (power loss)**

**input parameters ("accordion menus")**

**output field for results**

**download link for calculation report (PDF file)**

Results

temperature rise ≈ 44,4 K  
 contact temperature ≈ 124,4 °C  
 circumferential speed ≈ 12,6 m/s  
 thermal resistance ≈ 79,79 m·K/W

You can download a report containing your calculation results as a pdf file.

Download report

© 2023 University of Stuttgart

**Fig. 5: User interface of the web application IMA-InsECT**

(Fig.: University of Stuttgart)

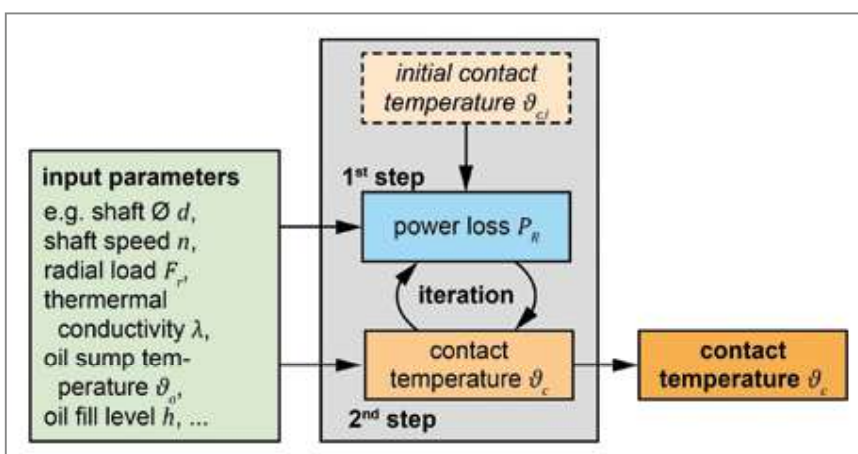


**Fig. 6: Iterative calculation consisting of two steps**

(Fig.: University of Stuttgart)

temperature itself, both steps are repeated iteratively. By default, 100 iterations are executed, so that the calculated temperature finally does not change significantly any longer (change much lower than 0.01 K).

Separating the calculation into two steps allows for a modular approach. There are four methods for calculating the temperature rise and three methods for determining the power loss integrated in IMA-InsECT. The user can choose for each step the method that is best-suited for his application. In the following, one calculation method for the temperature rise and one for the frictional heat are briefly presented. Both methods are robust as well as versatile [22]. All other calculation methods implemented in IMA-InsECT are described in [22] and [26].

### Calculating the temperature rise using the ExACT method

The ExACT method (Extended Approximation of the Contact Temperature of Rotary Shaft Seals) is based on a thermal model of the sealing system. The approach is physically-based and is similar to the Upper method [27] with some more simplifications (e.g. heat transfer to the air side) (Fig. 7).

The central component of the ExACT method is the thermal resistance, which is defined as the ratio of the temperature/ $\vartheta_o$  difference between the contact area (temperature/ $\vartheta_c$ ) and the oil sump (temperature  $\vartheta_o$ ) and the specific power loss (which is the absolute power loss related to the shaft circumference/ $\pi d$ ),

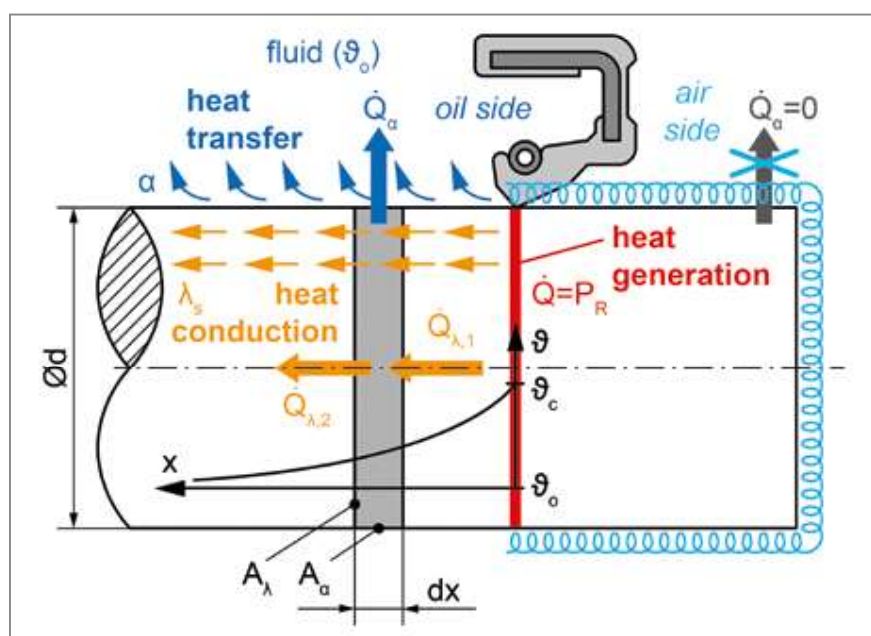


Fig. 7: Thermal model of the sealing system used in the ExACT method

(Fig.: University of Stuttgart)

$$R_o = \frac{\Delta\vartheta}{\frac{P_R}{\pi d}} = \frac{\vartheta_c - \vartheta_o}{\frac{P_R}{\pi d}}. \quad \text{Eq. 2}$$

The thermal resistance describes the capability of the sealing system to transfer the generated heat from the contact area away to the environment. It is a parameter of the sealing system, its operating parameters (e.g. oil fill level) and its environment. In contrast to the temperature difference  $\Delta\vartheta$ , the thermal resistance can be used to describe the heat transfer independent of the heat generation. Thus, the thermal resistance allows to compare sealing systems only with respect to the heat transfer. Low values for indicate a good heat transfer, high values indicate a restricted heat transfer to the environment.

Using the thermal resistance, the contact temperature can be calculated for a given combination of power loss and oil sump temperature,

$$\vartheta_{c,EXACT} = \vartheta_o + \Delta\vartheta_{EXACT} = \vartheta_o + R_o \cdot P_R / \pi d. \quad \text{Eq. 3}$$

Balancing the heat fluxes for the thermal model of the sealing system, an analytical solution for calculating the thermal resistance can be obtained,

$$R_o = 2 / \sqrt{(\lambda_s \cdot Nu \cdot \bar{\lambda}_o)}. \quad \text{Eq. 4}$$

This equation contains 3 parts:

- The thermal conductivity of the shaft material  $\lambda_s$  describes the heat conduction in the shaft. A comprehensive collection of values for typical shaft materials can be found in [28] and [29].
- The Unfelt number  $Nu$  describes the convective heat transfer between the shaft and the oil. This number is calculated using an empirical correlation to the Reynolds number, where the coefficients are determined by a conjugate heat transfer simulation (CHT) [30].
- The thermal conductivity of the air-oil mixture  $\bar{\lambda}_o$  describes the heat conduction on the oil side. Often, the shaft is surrounded on the oil side not only by oil but also by air. To consider for such multiphase flows, an effective thermal conductivity  $\bar{\lambda}_o$  is calculated by averaging,

$$\bar{\lambda}_o = h_{rel} \lambda_{oil} + (1 - h_{rel}) \lambda_{air}. \quad \text{Eq. 5}$$

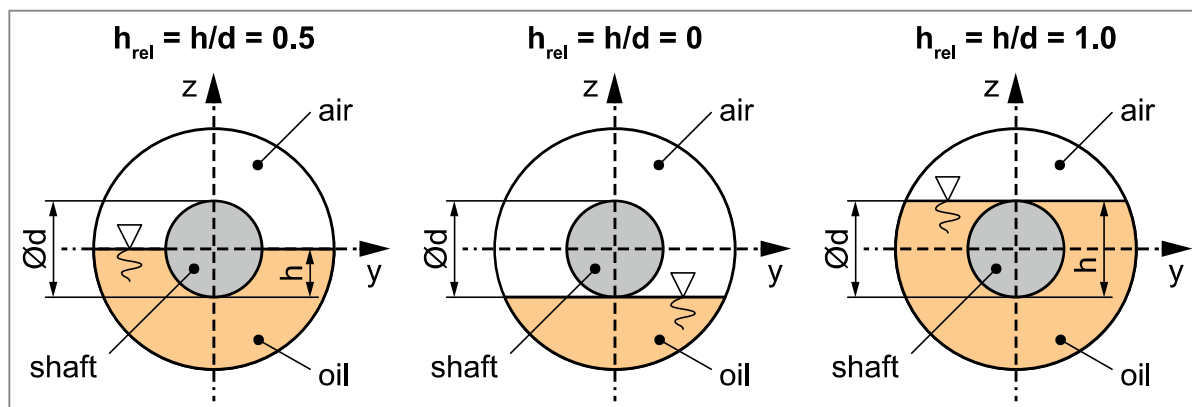


**Fig. 8: Definition of the relative oil fill level** (Fig.: University of Stuttgart)

The values of oil  $\lambda_{oil}$  and air  $\lambda_{air}$  are weighted with the relative oil fill level  $h_{rel} = h/d$ . The relative oil fill level is measured from the lower edge of the shaft and related to the shaft diameter (**Fig 8**). The relative oil fill level can have values between 0 and 1.

The ExACT method can be modified to take heat transfer to the air side into account. The lower the ambient temperature  $\vartheta_a$  at the air side (compared to the temperature on the oil side  $\vartheta_o$ ), the larger the proportion of the heat transfer toward the air side. Thus, this temperature difference (multiplied with a coefficient  $K_a$  is used to modify (**Eq. 3**) in order to consider the heat transfer to the air side in. Additionally, the thermal resistance representing the heat transfer to the oil side is modified by a correction factor  $K_o$ ,

$$\vartheta_{c,ExACT,mod} = \vartheta_o + \Delta\vartheta_{ExACT,mod} = \vartheta_o + K_o \cdot R_o \cdot \frac{P_R}{\pi d} - K_a (\vartheta_o - \vartheta_a). \quad \text{Eq. 6}$$

The coefficients  $K_a$  and  $K_o$  consider the air- and oil-side periphery of the sealing system and are application-specific. They can be determined by linear regression based, for example, on simulation results [30]. Typical values are in the range of  $K_o \approx 1.03$  and  $K_a \approx 0.07$ . The mentioned values are used as default parameters in IMA-InsECT. However, there are some applications where it is possible or even better to neglect the heat transfer to the air side. For example, in applications with additional heat sources and/or very high air temperatures. In these cases, the heat transfer towards the air side can be neglected by choosing  $K_o = 1.0$  and  $K_a = 0$ .

### Temperature dependant properties

The viscosity of many fluids strongly decreases with increasing temperature. The viscosity-temperature behaviour can be described by the Ubbelohde-Walther equation in terms of the kinematic viscosity  $\nu$  in  $\text{mm}^2/\text{s}$  and the absolute temperature  $T$  in Kelvin. The two material specific coefficients  $K_\nu$  and  $m$  can be obtained by two values of the





kinematic viscosity at two different temperatures (e.g. 40 and 100 °C which are often specified in the technical data sheets), see standards DIN 51563 [31] and DIN 53017 [32],

$$\lg(\lg v + 0.8) = K_v - m \cdot \lg T. \quad \text{Eq. 7}$$

The dynamic viscosity can be calculated by multiplying the kinematic viscosity  $v$  and the density  $\rho$  of the oil, which can also be modelled as a function of temperature according to DIN 51757 [33],

$$\eta(\vartheta) = v(\vartheta) \cdot \rho(\vartheta). \quad \text{Eq. 8}$$

The radial load  $F_r$  of rotary shaft seals decreases with increasing temperature [21]. This behaviour can be modelled by a linear function, where a coefficient  $\alpha_{Fr}$  indicates how many Newtons the radial load decreases with a temperature increase of 1 Kelvin. Using this approach, the radial load can be calculated for every desired temperature  $\vartheta$  that differs from room temperature  $\vartheta_{RT}$ ,

$$F_r(\vartheta) = F_r(\vartheta_{RT}) - \alpha_{Fr} (\vartheta - \vartheta_{RT}). \quad \text{Eq. 9}$$

The coefficient  $\alpha_{Fr}$  can be determined by measuring the radial load at two different temperatures using a measuring device with temperature chamber [34]. If the temperature effect is not known, a constant radial load can be assumed ( $\alpha_{Fr} = 0$  N/K) which makes the result less accurate.

To obtain realistic values of the radial load, not only the temperature but also time effects of the visco-elastic material behaviour should be considered. Thus, the seals should be stored for 24 hours on a mandrel before measurement in order to allow for stress relaxation in the elastomer material of the sealing lip [34].

### Calculating the frictional heat using the Guembel curve friction model

There are several methods for calculation the friction heat which is required as an input parameter by the ExACT method, (Eq. 6). For this purpose, often the so called Guembel curve friction model is used. This model is based on the Guembel curve representing an empirical relation between the lubrication and the friction condition of a sealing system. Both conditions are described by dimensionless numbers.

The lubrication condition of the sealing system is described by the Guembel number, that contains the dynamic viscosity  $\eta$  of the fluid in the sealing gap, the angular

velocity  $\omega$  of the shaft and the average contact pressure  $p_m$  in the sealing contact between sealing edge and shaft,

$$G = (\eta \cdot \omega) / p_m \quad \text{Eq. 10}$$

To obtain the effective viscosity in the sealing gap, the contact temperature  $\vartheta_c$  must be used to determine the dynamic viscosity. In the same way, it is recommended to use the radial load at oil sump temperature  $\vartheta_o$  (which represents the average temperature in the sealing lip and membrane) for calculating the average contact pressure in the contact area with size  $A = \pi db$ ,

$$G = \frac{\eta(\vartheta_c) \cdot \omega}{\frac{F_r(\vartheta_o)}{\pi db}} \quad \text{Eq. 11}$$

The coefficient of friction describes the friction condition and is defined as the ratio of the frictional force to the normal force. The frictional force  $F_R$  can be determined by dividing the frictional torque  $M_R$  by half the shaft diameter  $d/2$  representing the lever arm. As normal force, it is most convenient to use the radial load at room temperature  $\vartheta_{RT}$

$$\mu = \frac{F_R}{F_r} = \frac{2 \cdot M_R}{d \cdot F_r(\vartheta_{RT})} \quad \text{Eq. 12}$$

**Fig. 9** shows an exemplary Guembel curve for a specific sealing system based on measurements of the frictional torque on a test rig. The relation between the Guembel number and the coefficient of friction can be approximated using a quadratic function [18],

$$\mu(G) = A_1 \cdot (\lg G + A_2)^2 + A_3 \quad \text{Eq. 13}$$

The empirical relation (that means the 3 parameters  $A_1$ ,  $A_2$  and  $A_3$ ) is only valid for identical sealing systems and cannot be transferred to other sealing systems where one or more components of the sealing system (seal ring, shaft, oil) are changed. Just by changing the shaft surface, the Guembel curve can be varied by a factor of 3 [35]!

After calculating the coefficient of friction based on the Guembel curve, the power loss can be calculated which equals the generated heat that has to be transferred away from the sealing contact.





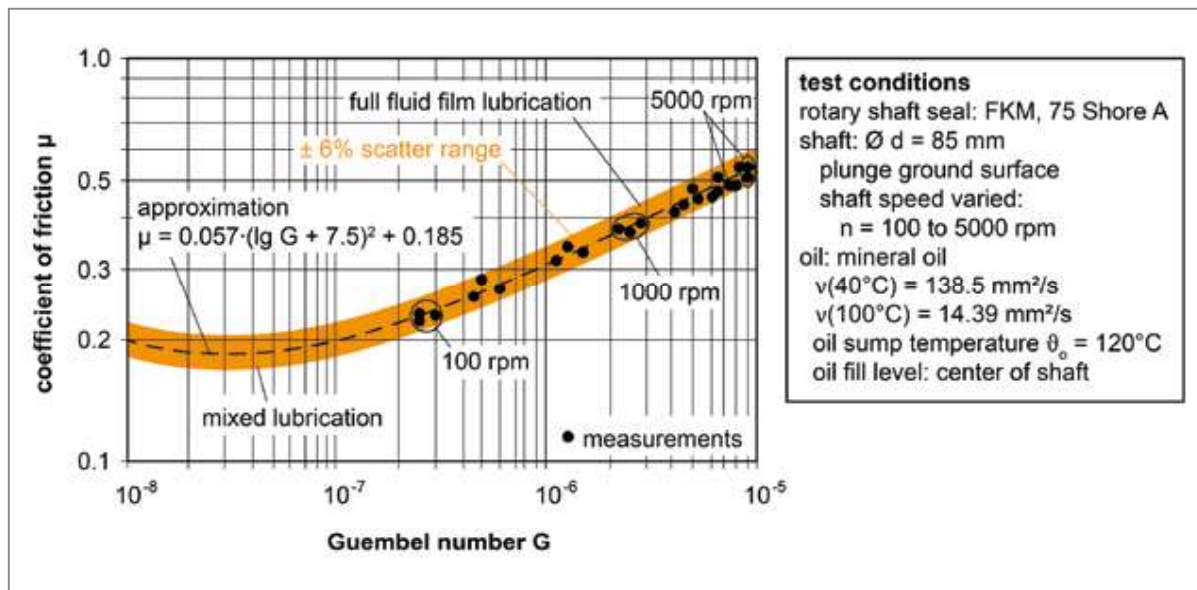


Fig. 9: Exemplary Guembel curve [17] (Fig.: University of Stuttgart)

$$P_R = \omega \cdot M_R = \pi \cdot n \cdot d \cdot \mu(G) \cdot F_r (\vartheta_{RT}) \quad \text{Eq. 14}$$

Here, it is important to use the same radial load as for calculation the coefficient of friction (e.g. radial load at room temperature  $\vartheta_{RT}$ ).

Combining this Guembel curve friction model for estimating the power loss (which equals the generated heat) with the ExACT method for calculation the temperature rise allows for an iterative solution of both quantities. Each result is used as a new input for the following calculation of the other quantity. The iterative solution is done automatically by IMA-InsECT which returns the final result within a fraction of a second. In addition to the two default calculation models recommended by the developers and presented in this work, IMA-InsECT offers other popular calculation models which can be combined due to its modular approach.

### Calculation of the pumping rate with the web application

The pumping rate is calculated using an empirical relation based on pumping rate measurements with rotary shaft seals, plunge ground shaft sleeves made of 100Cr6 and additive-free reference oils defined by the research association FVA (German Research Association for Drive Technology) [36]. The pumping rate measurements were performed within 2 research projects ([10] and [12]) and carried out with an inversely mounted seal ring (test duration 10 h, oil sump temperature 40 °C) for 6 different oil-elastomer combinations given in **Tab. 1**. Fluoro and nitrile elastomer compounds were combined with mineral and synthetic (polyalphaolefin and polyglycol) oils.

The empirical relation of the pumping rate takes the following 4 system parameters into account: the shaft diameter, the roughness of the shaft surface, the circumferential speed of the shaft and the dynamic viscosity of the oil at 40 °C. The variation range of the individual system parameters is given in **Tab. 2**.

The system parameters were varied by the DoE approach (Design of Experiments) for each oil-elastomer combination. The measurement data were analysed by regression analysis using a multiple quadratic polynomial. The multiple quadratic regression polynomial with the four system parameters corresponds to **Eq.15**. Here,  $c_0$  to  $c_{44}$  are the 15 coefficients to be determined by least squares method,  $R_z$  is the parameter for the surface roughness,  $u$  is the circumferential speed,  $\eta$  is the dynamic viscosity at oil sump temperature and  $d$  is the system diameter.

FVA reference oil [36]		Elastomer compound and rotary shaft seal type [37]	
Base oil type	Oil name [36]	Fluoro elastomer 75 FKM 585	Nitrile elastomer 72 NBR 902
Mineral oil	FVA No. 1, 2, 3 and 4	BAUMX7 (trimmed sealing edge)	BAFUDX7 (moulded sealing edge)
Polyalphaolefin oil (synthetic)	FVA PAO No. 1, 3 and 4	BAUMX7 (trimmed sealing edge)	BAUX2 (trimmed sealing edge)
Polyglycol oil (synthetic)	FVA PG No. 1, 3 and 4	BAUMX7 (trimmed sealing edge)	BAUX2 (trimmed sealing edge)

**Tab. 1: Oil-elastomer combinations for the pumping rate model** (Source: University of Stuttgart)

System parameter	Variation range
Shaft diameter	20 to 100 mm
Roughness of the shaft surface: Mean roughness depth $R_z$	1 to 7 $\mu\text{m}$ for mineral oil 2 to 5.3 $\mu\text{m}$ for synthetic oil
Circumferential speed	1 to 12 m/s for nitrile elastomer 1 to 28 m/s for fluoro elastomer
Dynamic viscosity of the oil at 40 °C	12 to 405 mPa·s for mineral oil (FVA) 23 to 338 mPa·s for polyalphaolefin oil (FVA PAO) 72 to 480 mPa·s for polyglycol oil (FVA PG)

**Tab. 2: Variation range of the individual system parameters** (Source: University of Stuttgart)



$$\begin{aligned}
 \text{pumping rate} = & \left[ \underbrace{c_0}_{\text{constant}} + \underbrace{c_1 \cdot Rz + c_2 \cdot u + c_3 \cdot \eta + c_4 \cdot d}_{\text{main effects}} \right. \\
 & + \underbrace{c_{12} \cdot Rz \cdot u + c_{13} \cdot Rz \cdot \eta + c_{14} \cdot Rz \cdot d + c_{23} \cdot u \cdot \eta + c_{24} \cdot u \cdot d + c_{34} \cdot \eta \cdot d}_{\text{interactions}} \\
 & \left. + \underbrace{c_{11} \cdot Rz^2 + c_{22} \cdot u^2 + c_{33} \cdot \eta^2 + c_{44} \cdot d^2}_{\text{quadratic effects}} \right]^2 \quad \text{Eq. 15}
 \end{aligned}$$

The regression polynomial contains linear terms to describe the main effects of the individual system parameters, terms with two system parameters to describe the interactions between the system parameters, and quadratic terms to account for the nonlinear effects. Interactions occur when the change in one system parameter also changes the effect of another parameter. An effect can be strengthened or weakened by interactions. There is a regression polynomial for each of the 6 oil-elastomer combinations.

The pumping rate is given in three units by IMA-InsECT: as pumping rate per sliding distance, per revolution and per time. Additionally, a report as PDF file is provided, containing 4 curves showing the pumping rate as a function of each individual system parameters and the appropriate confidence regions (**Fig. 10**). Due to the interactions between the individual parameters, the pumping rate curves shown in the Report must not be assumed to be static. If one system parameter is varied, the curves for the other three parameters change.

### Summary and Conclusion

IMA-InsECT allows for estimating the contact temperature of rotary shaft seals based on the most relevant operating conditions and system parameters. Thus, engineers are able to evaluate the risk of thermal damaging. Furthermore, IMA-InsECT can be used to analyse the influence of any single operating condition and system parameter and thus to evaluate the effect of optimisation steps. The web application offers a modular approach with several calculation methods for the temperature rise and the power loss which are calculated iteratively in most cases. As default, the physically-based ExACT method is used for calculating the temperature rise and the empirical Guembel curve friction model for estimating the power loss that equals the frictional heat. The combination of these two versatile methods is applicable to a broad variety of applications [22].

In addition to calculating the contact temperature, it can also be used for estimating the pumping rate of rotary shaft sealing systems. The pumping rate calculation in the web application is based on an empirical model that contains 4 important system parameters:

## Pumping rate - calculation report

Pumping rate calculation with: FKM, BAUMX7, Sealing edge trimmed, Polyalphaolefin oil

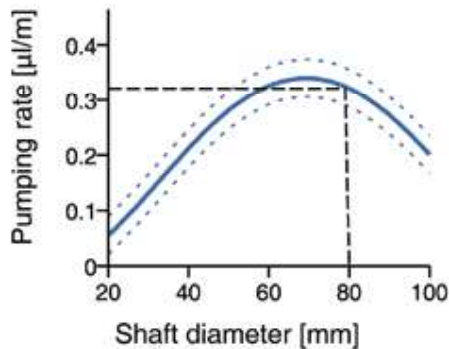
### Operating conditions:

shaft diameter [mm]: 80.0  
 mean roughness depth Rz [ $\mu\text{m}$ ]: 2.5  
 circumferential speed [m/s]: 5.0  
 dynamic viscosity [mPa·s]: 200.0

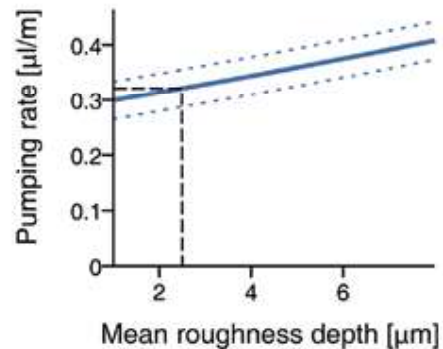
### Results:

Pumping rate per distance unit  $\approx 0.321 \mu\text{l/m}$   
 Pumping rate per revolution  $\approx 0.008 \mu\text{l/U}$   
 Pumping rate per time unit  $\approx 5.785 \text{ ml/h}$

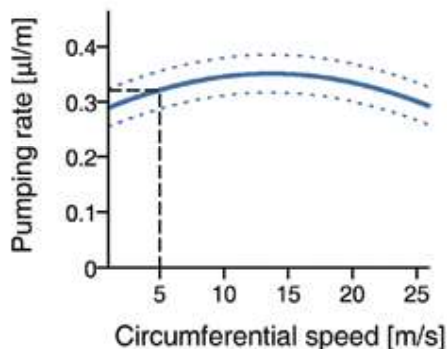
#### Diameter influence



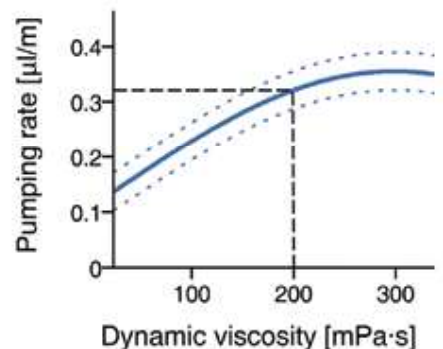
#### Roughness influence



#### Speed influence



#### Viscosity influence



— Characteristic    ····· Confidence region    - - - - - Operating point

Due to the interactions between the individual parameters, the pumping rate curves shown here as a function of the individual system parameters must not be assumed to be static. If one system parameter is varied, the curves for the other three parameters change.

Fig. 10: Report of pumping rate calculation (Fig.: University of Stuttgart)



- the system diameter,
- the circumferential speed,
- the surface roughness of the shaft and
- the dynamic viscosity of the fluid to be sealed.

The empirical model describes the influence of the parameters with a quadratic polynomial as well as the interactions of the parameters. Empirical models for 6 oil-elastomer combinations were determined based on pumping rate measurements performed with mineral and synthetic (PAO and PG) oils in combination with rotary shaft seals made of nitrile and fluoro elastomer. Thus, the pumping rate can be estimated for many applications.

### Acknowledgement

The Authors would like to thank Mr. Benjamin Schnabel for his long-term support as a student assistant in the development of the web application IMA-InsECT.

### Literature

- [1] Müller, H. K.; Nau, B. Fluid Sealing Technology - Principles and Applications. New York : Dekker, 1998.
- [2] Horve, L.: Shaft Seals for Dynamic Applications. New York : Dekker, 1996.
- [3] Bauer, F.: Tribologie. prägnant und praxisrelevant. Springer Vieweg, 2021. ISBN 978-3-658-32919-8.
- [4] DIN 3760. Rotary shaft lip type seals. September 1996. (in German)
- [5] DIN 3761. Rotary shaft lip type seals for automobiles. 15 Parts. November 1983 to January 1984. (in German, withdrawn in March 2017)
- [6] ISO 6194. Rotary shaft lip-type seals incorporating elastomeric sealing elements. 5 parts. September 2007 to November 2009.
- [7] Feldmeth, S.; Braeuer, P.; Franke, J.; Bauer, F.: Temperature measurement in the sealing contact – Sealing systems are getting smarter. XXII. Dichtungskolloquium. Vulkan. Steinfurt/Münster 9/2021, p. 15-26, ISBN 978-3-8027-2240-0.
- [8] Bauer, F.: Federvorgespannte Elastomer-Radial-Wellendichtungen. Grundlagen der Tribologie & Dichtungstechnik, Funktion und Schadensanalyse. Springer Vieweg, 2021. ISBN 978-3-658-32921-1.
- [9] Remppis, M.; Bauer, F.; Haas, W.: Measurement of the Pump Rate of Radial Lip Seals During Long Term Tests. Proceedings of the VII. Iberian Conference on Tribology (IBERTRIB), Porto, Portugal, June 20-21 2013, ISBN 978-972-752-156-2.
- [10] Remppis, M., Bauer, F., Haas, W.: Rechnerische Abschätzung der Dichtgüte von Radial-Wellendichtungen durch Kenntnis der Systemparametereinflüsse. Abschlussbericht, FVA-Forschungsvorhaben Nr. 617 I / IGF-Nr. 16402N, FVA-Heft 1066, Frankfurt/Main 2013
- [11] Remppis, M.: Untersuchungen zum Förderverhalten von Dichtsystemen mit Radial-Wellendichtungen aus Elastomer. PhD thesis. University of Stuttgart, 2016. ISBN: 978-3-936100-68-6.



- [12] Bekgulyan, S.; Bauer, F.; Haas, W.: Rechnerische Abschätzung der Dichtgüte von Radial-Wellendichtungen durch Kenntnis der Systemparametereinflüsse II. Abschlussbericht, FVA, Forschungsvorhaben Nr. 617 II, FVA-Heft 1259, IGF-Nr. 17938 N/1, Frankfurt/Main, August 2017.
- [13] Bekgulyan, S.; Feldmeth, S.; Bauer, F.: Influence of static and dynamic eccentricity on the pumping rate of radial lip seals. 25th International Conference on Fluid Sealing, BHR Group, Manchester, March 4-5 2020, pp. 79-91, ISBN: 978-1-85598-177-5.
- [14] Bekgulyan, S.; Feldmeth, S.; Bauer, F.: Influence of Low Temperature on the Pumping Rate of Radial Lip Seals. Machine and Industrial Design in Mechanical Engineering. KOD 2021. Mechanisms and Machine Science, vol. 109. Springer, 2022, ISBN 978-3-030-88464-2 / 978-3-030-88465-9, DOI: [https://doi.org/10.1007/978-3-030-88465-9\\_12](https://doi.org/10.1007/978-3-030-88465-9_12)
- [15] Bekgulyan, S.; Feldmeth, S.; Bauer, F.: Influence of dynamic eccentricity on the pumping rate of rotary shaft seals at sub-zero temperatures. 21st International Sealing Conference (ISC), Stuttgart, October 12-13, 2022; Fachverband Fluidtechnik im VDMA e.V., 2022, p. 133-146, ISBN 978-3-8163-0756-3
- [16] Daubner, A.; Haas, W.: Simulation of the temperature in and in front of the friction contact. NAFEMS Seminar: Simulation of complex flows - Applications and trends. 2009. ISBN 978-1-874376-58-3.
- [17] Jung, S.; Daubner, A.; Haas, W.: Measurement and Simulation of Two-Phase Flow in Sealing Application. 16th International Sealing Conference (ISC), Stuttgart 2010. pp. 303-316. ISBN 978-3-00-03523-6.
- [18] Feldmeth, S.; Bauer, F.; Haas, W.: Analysis of the Influence of Different Test Rig Setups on the Contact Temperature of Radial Lip Seals by Conjugate Heat Transfer Simulation. NAFEMS World Congress 2013. Salzburg, Austria. ISBN 978-1-87-4376-91-0.
- [19] Kunstfeld, T.; Haas, W.: Dichtungsumfeld: Einfluss des bespritzungs- und luftseitigen Umfeldes auf die Dichtwirkung von Radial-Wellendichtungen. FKM-Forschungsheft 261, Frankfurt/Main 2001.
- [20] Bauer, Frank; Haas, W.: Radial Lip Seal Contact Temperature - Influence of Different Test Rig Setups. ICEM 15, Porto, Portugal, 2012, Proceedings of the 15th ICEM, Gomes, Vaz (Editors), ISBN 978-972-8826-25-3
- [21] Feldmeth, S.; Olbrich, C.; Bauer, F.: Influence of Lubricants on the Thermal Behaviour of Rotary Shaft Seals. 21st International Sealing Conference (ISC), Stuttgart, October 12-13, 2022; Fachverband Fluidtechnik im VDMA e.V., 2022, p. 147-161, ISBN 978-3-8163-0756-3
- [22] Feldmeth, S.; Bauer, F.; Haas, W.: Abschätzverfahren für die Kontakttemperatur bei Radial-Wellendichtungen. 19th International Sealing Conference (ISC), Stuttgart, October 12-13, 2016; Fachverband Fluidtechnik im VDMA e.V., 2016, p. 122-137, ISBN 978-3-8163-0684-9, DOI: <http://dx.doi.org/10.18419/opus-11873>
- [23] University of Stuttgart, Institute of Machine Components (IMA): InsECT. <https://insect.ima.uni-stuttgart.de/>
- [24] Django Software Foundation: Django – The web framework for perfectionists with deadlines. <https://www.djangoproject.com/>
- [25] Bootstrap – The most popular HTML, CSS, and JS Library in the world. <https://getbootstrap.com/>



- [26] Feldmeth, S.; Bauer, F.; Haas, W.: Abschätzung der Kontakttemperatur bei Radial-Wellendichtungen mit der selbstentwickelten Open-Source-Software InsECT. Schweizer Maschinenelemente Kolloquium SMK 2016. November 22-23, 2016, Rapperswil, Schweiz; KISSsoft AG (edt.); TUDpress, 2016 – ISBN 978-3-95908-065-1
- [27] Upper, G.: Dichtlippentemperatur von Radial-Wellendichtringen : Theoretische und experimentelle Untersuchungen. PhD thesis. Universität Karlsruhe, 1968.
- [28] VDI-Gesellschaft Verfahrenstechnik und Chemieingenieurwesen (Hrsg.): VDI-Wärmeatlas. 11. Auflage. Springer Vieweg, 2013. <https://doi.org/10.1007/978-3-642-19981-3>.
- [29] Richter, F.: Die physikalischen Eigenschaften der Stähle. Das 100 Stähle Programm. 2011. [https://www.tugraz.at/fileadmin/user\\_upload/Institute/IEP/Thermophysics\\_Group/Files/Staehle-Richter.pdf](https://www.tugraz.at/fileadmin/user_upload/Institute/IEP/Thermophysics_Group/Files/Staehle-Richter.pdf). Last Access: 2023-07-12.
- [30] Feldmeth, S.; Bauer, F.; Haas, W.: Bestimmung von Kennzahlen für die Temperaturüberhöhung bei Radial-Wellendichtungen mittels CHT-Simulation. ANSYS Conference & 33th CADFEM Users' Meeting 2015, Bremen, June 24-26, 2015. ISBN 3-937523-12-X
- [31] DIN 51563: Testing of mineral oils and related materials. Determination of viscosity temperature relation. Slope m. April 2011. (in German)
- [32] DIN 53017: Viscometry. Determination of the temperature coefficient of viscosity of liquids. November 1993. (in German)
- [33] DIN 51757: Testing of mineral oils and related materials. Determination of density. January 2011. (in German)
- [34] Feldmeth, S.; Stoll, M.; Bauer, F.: How to measure the radial load of radial lip seals. Tribologie und Schmierungstechnik, Expert, Vol. 68, 3-4/2021, p. 5-12, ISSN 0724-3472. <https://doi.org/10.24053/TuS-2021-0014>
- [35] Jung, Steffen: Beitrag zum Einfluss der Oberflächencharakteristik von Gegenlaufflächen auf das tribologische System Radial-Wellendichtung. PhD thesis. University of Stuttgart, 2012.
- [36] Laukotka, E.: FVA-Heft 660. Referenzöle - Datensammlung. Forschungsvereinigung Antriebstechnik e.V. Frankfurt, 2007.
- [37] Freudenberg Sealing Technologies GmbH & Co. KG: Simmerring and rotary seals – Catalog (FNST) – Volume 11. Weinheim. 2015